ACS APPLIED ELECTRONIC MATERIALS

pubs.acs.org/acsaelm Article

# Low-Resistivity Titanium Nitride Thin Films Fabricated by Atomic Layer Deposition with $TiCl_4$ and Metal−Organic Precursors in Horizontal Vias

Cheng-Hsuan Kuo, Aaron J. Mcleod, Ping-Che Lee, James Huang, Harshil Kashyap, Victor Wang, SeongUK Yun, Zichen Zhang, Jeffrey Spiegelman, Ravindra Kanjolia, Mansour Moinpour, and Andrew C. Kummel*

Cite This: https://doi.org/10.1021/acsaelm.3c00245 Read Online

ACCESS | Metrics & More | Article Recommendations | Supporting Information

**ABSTRACT:** The resistivity of halogen-free atomic layer deposition (ALD) TiN thin films was decreased to 220 $\mu\Omega$ cm by combining the use of a high-thermal stability nonhalogenated Ti precursor with a highly reactive nitrogen source, anhydrous hydrazine ($N_2H_4$). TDMAT [tetrakis (dimethyl-amino)titanium], TDEAT [tetrakis(diethylamido)titanium], and TEMATi [tetrakis (ethylmethyl-amido)titanium] were compared to $TiCl_4$ as precursors for ALD TiN using $N_2H_4$ as a coreactant. By minimizing the pulse length of the Ti-source precursor and optimizing the deposition temperature, the resistivity of TiN thin films deposited using these precursors was reduced to 400 $\mu\Omega$ cm for TDMAT (at 350 °C), 300 $\mu\Omega$ cm TDEAT (at 400 °C), and 220 $\mu\Omega$ cm for TEMATi (at 425 °C) compared to 80 $\mu\Omega$ cm for $TiCl_4$ (at 500 °C). The data are consistent with the lowest resistivity for halogen-free ALD corresponding to the organic precursor with the highest thermal stability, thereby allowing maximum ALD temperature. After optimization, TiN thin films were grown in horizontal vias, illustrating conformal and uniform TiN using both $TiCl_4$ and TEMATi in horizontal vias in patterned substrates.

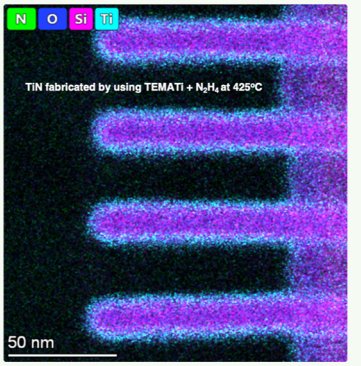


**KEYWORDS:** *thermal ALD, metal−organic precursors, TiN thin films, horizontal vias, low resistivity*



## INTRODUCTION

In semiconductors, TiN thin films that are conducting are utilized for several applications, including diffusion barrier liners for W, Co, and Cu,[1−4] barrier metals for high-density NAND flash memory devices,[5] and other 3D structures (especially re-entrant undercut structures) in which a metal diffusion barrier is needed, such as 3D NAND, 3D DRAM, gate all around (GAA) channels, and Si nanowire gate stacks.[6] TiN can also be utilized as a surface layer on carbon nanotubes in supercapacitors.[7] Low-resistivity TiN is currently deposited by PVD (physical vapor deposition, such as sputtering)[8] or ALD (atomic layer deposition) with $TiCl_4$ and $NH_3$.[9] However, as the scale of the transistors and devices shrinks to a couple of nanometers, halogen-free ALD will be ideal since it prevents metal corrosion.[10] For low-resistivity TiN thin films, a low concentration of impurities such as oxygen, carbon, and chlorine is required for low resistivity.[11] Plasma-enhanced ALD (PE-ALD) is typically employed to reduce resistivity by removing the surface impurities of the TiN films and by increasing TiN crystallinity. However, PE-ALD is not suitable for use in patterned substrates, such as those with horizontal vias, since ions neutralize and radicals recombine when in contact with substrate surfaces. Consequently, for TiN deposition in horizontal vias, thermal ALD is required.

Several ALD and CVD methods have been reported for depositing low-resistivity TiN thin films. Kröger et al. reported the synthesis of TiN using CVD (chemical vapor deposition) at 350 °C with a resistivity of 400 $\mu\Omega$ cm.[12] Stevens et al. presented the ALD growth of TiN on amorphous carbon.[13] Thermal ALD using $TiCl_4$ and $NH_3$ at 400 °C with a resistivity of ∼320 $\mu\Omega$ cm in an 18 nm film was reported by Elers et al.[14] Wolf et al.[15] reported thermal ALD using $TiCl_4$ and $NH_3$ as well as $TiCl_4$ and $N_2H_4$; for the $TiCl_4$ + $N_2H_4$ reaction at 400 °C, a resistivity of 359 $\mu\Omega$ cm was measured in an 11 nm film, which is lower than the 554 $\mu\Omega$ cm measured when using $TiCl_4$ with $NH_3$. In their work, it was reported that the resistivity of TiN can be reduced due to the higher reactivity of $N_2H_4$ compared to that of $NH_3$. Ahn et al. reported that high temperatures (500 °C) were required to deposit low-resistivity films using ALD with $TiCl_4$ and $NH_3$.[9] Lee et al.[16] reported a new ALD method to deposit TiN by using $TiCl_4$, $H_2S$, and

Received: February 24, 2023
Accepted: July 3, 2023

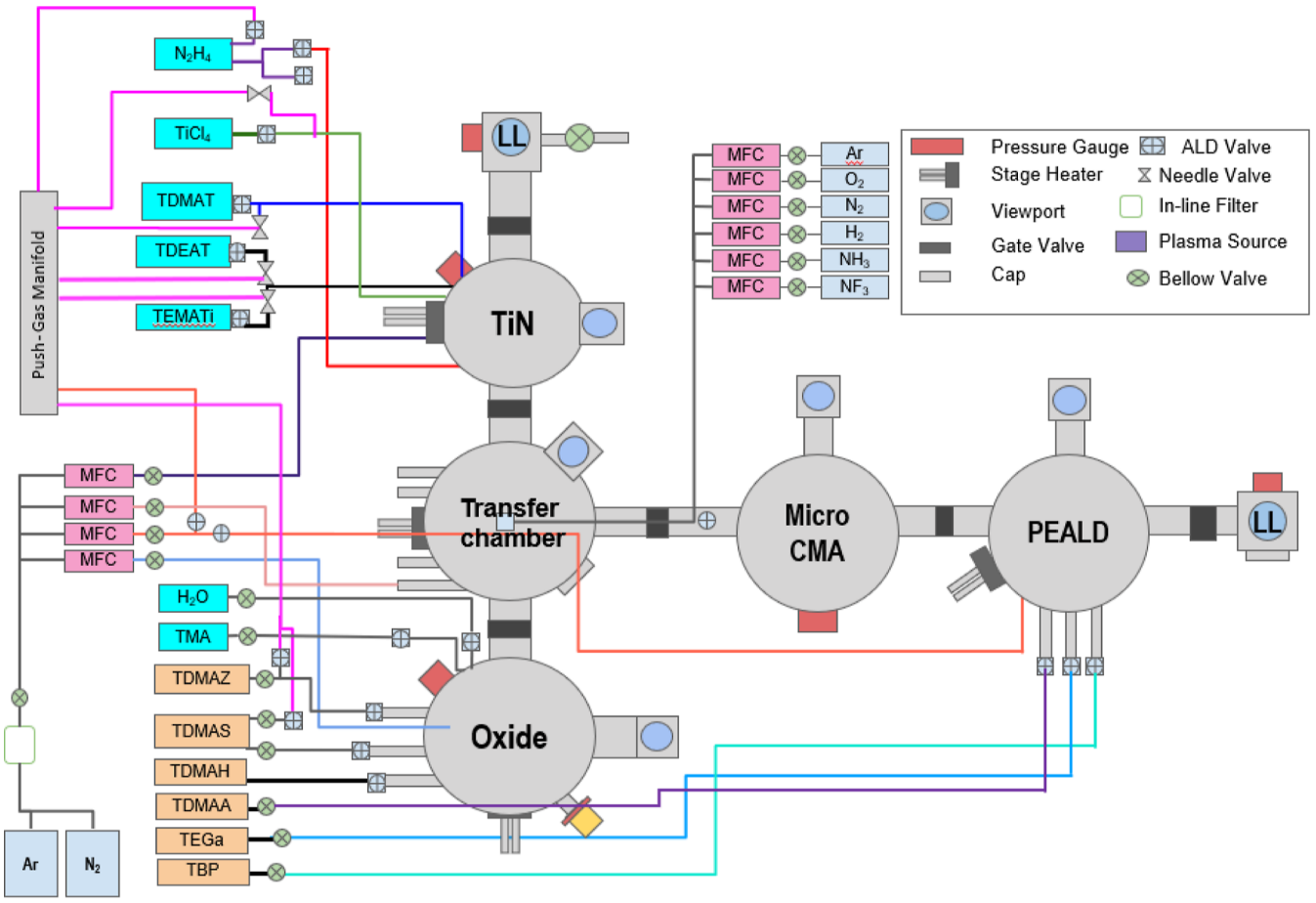


**Figure 1.** Configuration of the cluster tool. AES was connected to the nitride ALD chamber enabling measurement of the in situ chemical composition of the thin films without air exposure. Several precursors were connected to each chamber separately. A push-gas system was installed for the precursors with low vapor pressure such as TDEAT, TDMAT, and TEMTi.

$NH_3$. They reported TiN with a resistivity of ∼150 μΩ cm for a 12 nm film. However, $H_2S$ is a highly toxic precursor that is challenging to employ in semiconductor manufacturing. Elam et al.,[17] Wang et al.,[18] and Kim et al.[19] also published papers reporting TiN thin film ALD using other Ti precursors: TDMAT and TDEAT. In these reports, these halogen-free processes using organic precursors were considered promising compared to $TiCl_4$ since surface residual chlorine is corrosive. The resistivity of the TiN observed by Elam et al. was over 10 000 μΩ cm due to high oxygen content and low ALD temperature. Using TDEAT, Wang et al. reported lowering the resistivity of halogen-free ALD TiN to 450 μΩ cm in an 18.1 nm film. Besides thermal ALD, PEALD was also applied to synthesize TiN using TDMAT[20−22] and TEMATi[23] as precursors.

In the present study, thin films were grown by thermal ALD using titanium tetrachloride ($TiCl_4$) and organic precursors alongside anhydrous hydrazine ($N_2H_4$). For 425 °C $TiCl_4$ ALD, the resistivity of TiN thin films was 158 μΩ cm, while for 500 °C $TiCl_4$ ALD, the resistivity was reduced to 89 μΩ cm for a 15 nm film, which is comparable to the findings of Ahn et al. for a 30 nm film.[9] The lowest resistivities using TDMAT, TDEAT, and TEMATi ALD are 400, 295, and 220 μΩ cm, respectively, when used with $N_2H_4$ as a coreactant for ∼15 nm films; these correlated well with the maximum ALD temperatures. Benchmarking of TiN ALD techniques indicates that by using different Ti-source precursors, the resistivity of TiN thin films can be different. Conformal TiN (∼4 nm) thin films were grown by the thermal ALD process using $TiCl_4$ or TEMATi and $N_2H_4$ in horizontal vias in patterned samples.

## EXPERIMENTAL SECTION

300 nm thick $SiO_2$ grown on Si substrates provided by University Wafers was used to deposit TiN thin films, and the patterned substrates with the vertical trenches and horizontal vias were provided by Micron. A standard degreasing method was applied to clean the substrate before deposition, which consisted of quick rinses in acetone, methanol, and DI water for 1 min in each step. A high-purity nitrogen gun was used to remove the residual liquids or dust on the substrate before loading it into the load lock. Before transferring the substrate to the deposition chamber, a mechanical pump was utilized to reduce the pressure of the load lock to 0.1 Torr. The deposition chamber was pumped continuously by a turbopump at a base pressure as low as $1 \times 10^{-6}$ Torr. The chamber was heated to ∼130 °C to prevent the condensation of the precursor onto the side wall of the chamber. Note that this temperature is not so hot as to cause the decomposition of all metal−organic precursors.

For the nitrogen source, high-purity $N_2H_4$ (Rasirc, Brute Hydrazine) was used. This hydrazine source provides a stable, reliable flow of anhydrous hydrazine gas from a liquid source in a sealed vaporizer. The Brute hydrazine vaporizer converts source liquid hydrazine to gas while leaving behind the nonvolatile solvent. The maximum moisture content of $N_2H_4$ is less than 100 ppb. For the present study, the integrity of the $N_2H_4$ gas delivery system was confirmed by careful vacuum leak testing. A commercial $TiCl_4$ (Sigma-Aldrich) precursor was used as a Ti-source precursor. For


https://doi.org/10.1021/acsaelm.3c00245
ACS Appl. Electron. Mater. XXXX, XXX, XXX−XXX

metal−organic precursors, TDMAT [tetrakis(dimethylamino)-titanium], TDEAT [tetrakis(diethylamino)titanium], and TEMATi [tetrakis(ethylmethylamido)titanium] were provided by Sigma-Aldrich. A low-temperature ALD process was required for these halogen-free precursors to prevent decomposition. A push-gas system was installed for the metal−organic precursors. Ultrahigh-purity $N_2$ was passed through two purifiers: (a) an Entegris GateKeeper gas purifier was connected between the gas tank and the mass flow controller (MFC) and (b) another Entegris GateKeeper gas purifier was connected downstream of the MFC before the deposition chamber. The purified gas was employed for both the purge gas and push gas during the deposition. The flow rate of the purge gas was controlled by a MFC to ensure stable flow of the purge and push gas.

The deposition chamber was connected to an in situ Auger electron spectrometer (RBD Instruments) to determine the atomic composition of ALD TiN (See Figure 1). After the deposition in the nitride chamber, the samples were transferred in vacuum using a set of transfer arms to the AES chamber to measure the chemical composition and then to the PEALD chamber to perform the Ar plasma treatment at 300 °C and −100 V.

Ex situ atomic force microscopy (AFM) was used to characterize the surface roughness of the TiN thin films. The thicknesses of the TiN thin films were measured by X-ray reflectivity (XRR). The sheet resistances of the TiN thin films were measured using a four-point probe system (Ossila). With the thickness and sheet resistance of each thin film, the resistivity was calculated. Resistivity measurements were performed within 15 min of air exposure to minimize the oxidation of the TiN into $TiO_xN_y$, which is less conductive. A focused ion beam (FIB) was used for transmission electron microscopy (TEM) lamella preparation. During the process, Ir and Pt were deposited as protection layers. TEM was employed to check the conformality of the TiN thin films in the horizontal vias. Energy-dispersive X-ray spectroscopy (EDX) and electron energy loss spectroscopy (EELS) were used to analyze the composition of the thin films in the horizontal vias.

## RESULTS AND DISCUSSION

$TiCl_4$ + $N_2H_4$ was employed as a benchmark (process conditions are listed in Table 1) for the halogen-free processes,

**Table 1. Process Condition Matrix of TiN Using $TiCl_4$ with $N_2H_4$**[a]

| sample | $TiCl_4$ pulse lengths (ms) | $N_2H_4$ pulse lengths (ms) | temperature (°C) | GPC (Å) | resistivity ($\mu\Omega$ cm) |
|---|---|---|---|---|---|
| A-1 | 300 | 1200 | 425 | 1.62 | 274.06 |
| A-2 | 300 | 2400 | 425 | 1.65 | 237.62 |
| A-3 | 300 | 3600 | 425 | 1.94 | 162.96 |
| A-4 | 300 | 7200 | 425 | 1.98 | 158.96 |
| A-5 | 300 | 3600 | 500 | 1.95 | 89.08 |

[a]At first, the optimization of the precursor pulse length was conducted. Afterward, for sample A-5, a high-temperature process (~500 °C) was employed to compare to Ahn's result.

and ALD deposition temperature and pulse time optimization was performed for $TiCl_4$ + $N_2H_4$ (Figure 2). The $TiCl_4$ precursor bottle was maintained at room temperature. At first, TiN thin films were optimized at 425 °C. By increasing the pulse length of $N_2H_4$ from 1.2 to 3.6 s, the resistivity of TiN decreased, which correlated with a decrease in oxygen concentration. No significant effects of further increasing the $N_2H_4$ pulse length to 7.2 s were observed. To compare the result of Ahn et al., the deposition temperature was increased to 500. For 500 °C ALD, surface impurities such as oxygen and chlorine were comparable to the sample at 425 °C. However, the resistivity was reduced to less than 90 $\mu\Omega$ cm, which was comparable to Ahn's result. Low resistivity was ascribed to the

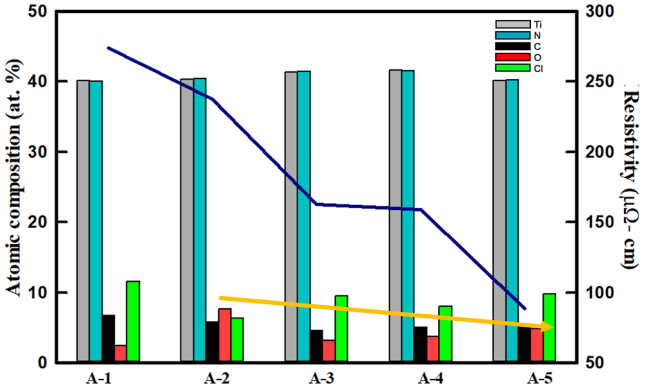


**Figure 2.** Pulse length study of TiN using $TiCl_4$ and $N_2H_4$. The pulse lengths of precursors were first optimized at 425 °C using both composition and resistivity as metrics (sample A-1−A-4). A minimum $N_2H_4$ of 3600 ms was required to minimize resistance and oxygen content. Afterward, high-temperature (500 °C) ALD was employed to further decrease resistivity (sample A-5). Note: the self-limitation study is shown in Supporting Information Figure S1. All the samples are in the saturated condition.

high deposition temperature (500 °C) and to low oxygen and carbon contamination allowing for the development of larger crystallites. Note that the resistivity was only constant for $N_2H_4$ pulse lengths greater than 3.6 s, consistent with the need for excess $N_2H_4$ to reduce O and Cl contaminants.

Postdeposition Ar plasma sputtering was utilized at 300 °C to remove the surface impurities such as chlorine (see Figure 3a) from 15 nm thick TiN samples deposited using $TiCl_4$ + $N_2H_4$ at 425 °C. AES shows that after 5 min of treatment, Cl was greatly reduced. This supports the hypothesis that these impurities are mainly on the surface. However, the Si signal located at ~90 eV was detected after Ar plasma treatment for 20 min, indicating that the thin film was overetched. Ar plasma is consistent with the 5 min treatment just removing a small surface layer containing no chlorine and reducing oxygen.

For the atomic hydrogen treatment shown in Figure 3b, the signal of Cl was significantly reduced after 5 min of treatment. However, it is observed that the oxygen content increased, probably due to the line of sight to the AES filament during the AES measurement or exposure to $H_2O$ during the sample transfer. Both surface treatments effectively decreased the Cl content in the thin films. This phenomenon is consistent with the hypothesis that Cl mainly existed on the surface of the thin films.

The deposition of TiN using TDMAT at 350 °C is shown in Figure 4 (process conditions are listed in Table 2); the low temperature was needed to prevent precursor decomposition that leads to carbon contamination. Typically, the TDMAT is stable at 200−300 °C.[24] In this work, the substrate temperature was maintained at a higher stage temperature to try to lower the resistivity of the thin films; inadvertent precursor decomposition was prevented by having a cold wall chamber. A cold wall chamber was employed to ensure minimal sample contamination by precursor decomposition products. For metal−organic precursors, long residence times on the walls of the chamber can lead to precursor decomposition and subsequent incorporation of decomposition products into the TiN films, thereby raising the resistivity. Note that the actual substrate temperature may be 30 °C below the stage temperature due to cooling by the purge gas. Samples (B-1−B-3 and B-5) were tested within the 10%


https://doi.org/10.1021/acsaelm.3c00245
ACS Appl. Electron. Mater. XXXX, XXX, XXX−XXX

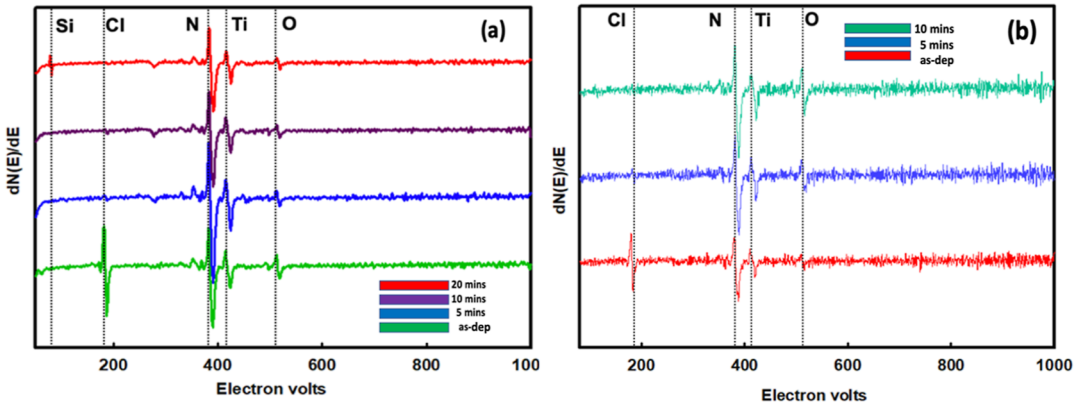


**Figure 3.** Postdeposition surface treatment using (a) Ar plasma at 50 W with a DC bias of −100 V and (b) atomic hydrogen treatment on ∼15 nm TiN thin films. The removal of surface impurities O and Cl was achieved after 5 min of Ar plasma treatment. The ratio of Ti to N was comparable to that of the as-dep sample. However, the Si substrate peak was observed after 20 min of treatment, indicating sputtering of the bulk TiN film. By using atomic hydrogen, the removal of surface impurity Cl was achieved after 5 min of treatment. However, the oxygen content was slightly increased, probably during the sample transfer. After atomic hydrogen treatment, the ratio of Ti to N was comparable to that of the as-dep sample. The starting 15 nm TiN films were prepared using $TiCl_4$ + $N_2H_4$ at 425 °C.

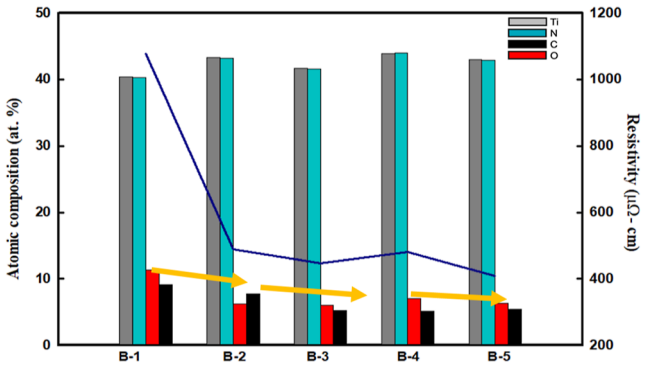


**Figure 4.** Pulse length study of TiN using TDMAT and $N_2H_4$. Due to the low thermal stability of the precursor, lower stage temperature (350 °C) as well as short TDMAT pulses were employed to avoid the decomposition of the precursor (yellow arrow). A minimum in carbon content and resistivity was observed by decreasing the TDMAT pulse length to 125 ms. Note: the self-limitation study is shown in Supporting Information Figure S1. B-4 was deliberately underdosed to test the resistivity.

**Table 2. Process Condition Matrix of TiN Using TDMAT with $N_2H_4$**[a]

| sample | TDMAT pulse lengths (ms) | $N_2H_4$ pulse lengths (ms) | temperature (°C) | GPC (Å) | resistivity ($\mu\Omega$ cm) |
|---|---|---|---|---|---|
| B-1 | 500 | 6000 | 350 | 1.59 | 1077.78 |
| B-2 | 250 | 6000 | 350 | 1.58 | 489.80 |
| B-3 | 125 | 6000 | 350 | 1.52 | 446.60 |
| B-4 | 30 | 6000 | 350 | 1.10 | 481.39 |
| B-5 | 60 | 6000 | 350 | 1.38 | 408.48 |

[a]Pulse length of TDMAT was optimized at a low temperature to avoid precursor decomposition. More ALD cycles were required for low-pulse length samples to deposit the same thickness (∼15 nm).

difference in the GPC, which means that they are saturated and can be corresponding to ALD. The pulse length of the TDMAT was decreased below the saturation point (as B-4) to test the resistivity. The self-limiting study is shown in the Supporting Information as Figure S1. The temperatures of the TDMAT precursor bottle and precursor line were also heated to 60 and 70 °C, respectively. At shorter TDMAT pulse lengths, the TiN resistivity was reduced due to decreased carbon and oxygen contents. Even for optimized pulse lengths, the surface oxygen and carbon for TDMAT-based films were greater than those for $TiCl_4$-based films.

TDEAT has higher thermal stability[25] and higher decomposition temperature (250 °C) than TDMAT, so it was tested at 350 and 400 °C, as shown in Figure 5 (process conditions

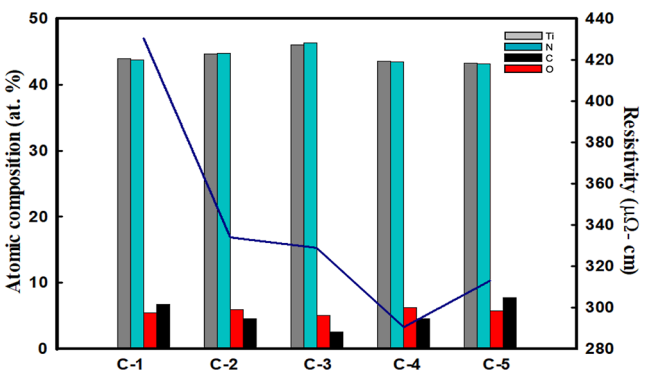


**Figure 5.** Pulse length and deposition temperature study of TiN using TDEAT and $N_2H_4$. The pulse length of the TDEAT precursor was optimized with a constant pulse length of $N_2H_4$ at different temperatures. A minimum in carbon content and resistivity was observed at 300 °C by decreasing the TDEAT pulse length to 150 ms However, the resistivity was further decreased by raising the stage temperature to 350 °C despite an increase in surface carbon content. Note: the self-limitation study is shown in Supporting Information Figure S1.

are listed in Table 3). The temperatures of the TDEAT precursor bottle and precursor line were also increased to 60 and 70 °C, respectively. While the TDEAT films had lower resistivity than the TDMAT films at 350 °C, the TDEAT film resistivity increased for the 400 °C deposition temperature due to the high carbon content, consistent with the decomposition of the TDEAT precursor at 400 °C (note the higher C content in sample C-5.)

The optimal metal−organic precursor was found to be TEMATi, as shown in Figure 6 (process conditions are listed in Table 4). The TEMATi precursor has the highest thermal stability and can be utilized at high temperatures at around 350


https://doi.org/10.1021/acsaelm.3c00245
ACS Appl. Electron. Mater. XXXX, XXX, XXX−XXX

**Table 3. Process Condition Matrix of TiN Using TDEAT with $N_2H_4$[a]**

| sample | TDEAT pulse lengths (ms) | $N_2H_4$ pulse lengths (ms) | temperature (°C) | GPC (Å) | resistivity ($\mu\Omega$ cm) |
|---|---|---|---|---|---|
| C-1 | 600 | 6000 | 350 | 1.42 | 430.59 |
| C-2 | 300 | 6000 | 350 | 1.40 | 334.05 |
| C-3 | 150 | 6000 | 350 | 1.38 | 329.01 |
| C-4 | 150 | 6000 | 350 | 1.37 | 290.44 |
| C-5 | 150 | 6000 | 350 | 1.38 | 312.92 |

[a]The pulse length of $N_2H_4$ remained constant at 6000 ms. The pulse length of the metal−organic precursor was gradually decreased to avoid precursor decomposition. The temperature was optimized to reach the lowest resistivity at 350 °C.

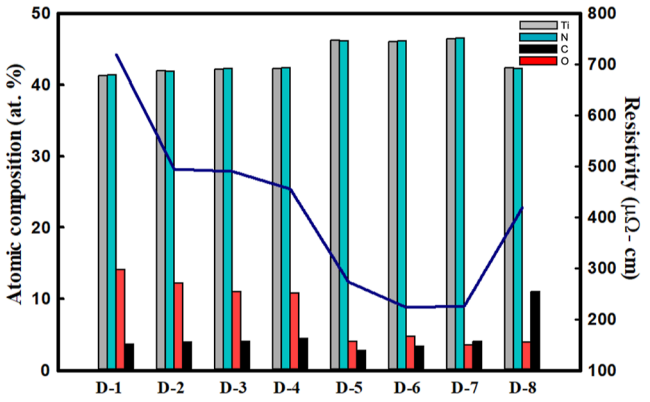


**Figure 6.** Pulse length and deposition temperature study of TiN using TEMATi and $N_2H_4$. The pulse lengths of both precursors were optimized at increasing temperatures to minimize the resistivity at each process temperature. As the stage temperature was increased, the lowest resistivity was observed with increasing $N_2H_4$ pulse length at 425 °C Note: the self-limitation study is shown in Supporting Information Figure S1.

**Table 4. Process Condition Matrix of TiN Using TEMATi With $N_2H_4$[a]**

| sample | TEMATi pulse lengths (ms) | $N_2H_4$ pulse lengths (ms) | temperature (°C) | GPC (Å) | resistivity ($\mu\Omega$ cm) |
|---|---|---|---|---|---|
| D-1 | 300 | 1200 | 300 | 0.90 | 720.11 |
| D-2 | 300 | 1200 | 350 | 1.06 | 495.02 |
| D-3 | 300 | 3600 | 350 | 1.01 | 490.03 |
| D-4 | 300 | 3600 | 400 | 1.08 | 456.21 |
| D-5 | 300 | 6000 | 400 | 1.11 | 276.61 |
| D-6 | 300 | 6000 | 425 | 1.09 | 223.72 |
| D-7 | 200 | 6000 | 425 | 1.08 | 226.72 |
| D-8 | 100 | 6000 | 450 | 0.98 | 415.34 |

[a]Pulse length and temperature optimization were performed to lower the resistivity. The TEMATi precursor will decompose at 450 °C, leading to higher carbon content and higher resistivity at 450 °C.

°C.[25] Therefore, the substrate temperature was increased from 300 to 450 °C. The precursor bottle and precursor line were at room temperature. To reach the lowest resistivity, optimization of the pulse lengths of both precursors was first conducted at 300 °C. No decomposition of TEMATi was observed at low temperatures, as indicated by the low carbon content. Consequently, stage temperatures were increased step by step until the carbon content in the thin films increased to 13%, resulting in high resistivity at 450 °C. As the stage temperature increased, the optimal pulse length of $N_2H_4$ increased for the lowest resistivity, consistent with the precursor-mediated chemisorption of $N_2H_4$. At 425 °C, the nucleation of the precursor was not saturated when the pulse length of TEMATi was decreased to 200 ms. Therefore, sample F was designated as the optimized condition at 425 °C.

A comparison of resistivity for TiN using $TiCl_4$ as well as metal−organic precursors is shown in Figure 7. When the

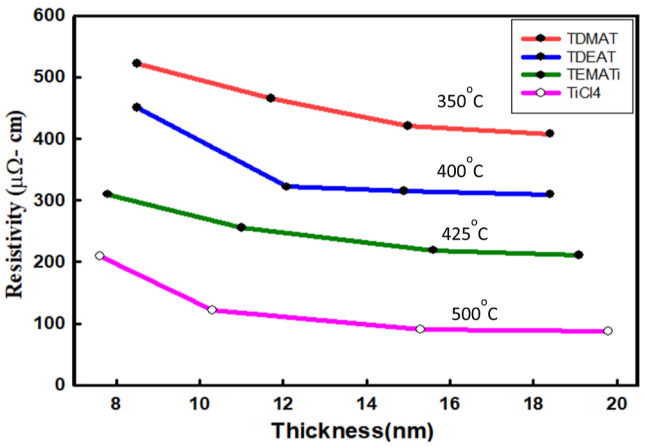


**Figure 7.** Comparison of resistivity for TiN using $TiCl_4$ as well as metal−organic precursors. TDMAT (in red) was employed for ALD at 350 °C to avoid the decomposition of the precursor. With higher thermal stability, TDEAT and TEMATi can be used at higher ALD temperatures of 400 and 425 °C, respectively. For $TiCl_4$, the lowest resistivity (~89 mΩ cm) can be achieved at 500 °C ALD temperature. All the precursors show the same trend, that is, as the thickness of the film increases to 15 nm, the resistivity is saturated.

thickness of the thin films reached ~15 nm, the resistivity was minimized. Among all metal−organic precursors, TEMATi produced films with the lowest resistivity, ~220 $\mu\Omega$ cm, consistent with the relatively high thermal stability of the precursor enabling a deposition temperature of 425 °C. It is hypothesized that the crystallinity of deposited TiN using TEMATi could be improved relative to those deposited using TDEAT or TDMAT due to the higher process temperature while still minimizing carbon incorporation. As shown in Figure S2, TiN thin films using both precursors become denser at a higher temperature consistent with a more crystalline grain structure, leading to a decrease in resistivity. Surface RMS roughness also increases at higher process temperatures consistent with more crystalline grain structures. It is noted that the residual carbon and oxygen in the optimized 425 °C TEMATi + $N_2H_4$ films were comparable to those in the optimized $TiCl_4$ + $N_2H_4$ films at 425 °C ALD temperature.

As shown in Figure 8, the resistivity increased below 15 nm; this is consistent among all precursors since the top 2−3 nm of the surfaces were oxidized by air exposure. It is also possible that the thinner films had more surface scattering, thereby increasing resistivity.[26] For $TiCl_4$, the resistivity was reduced to ~90 $\mu\Omega$ cm with the 500 °C ALD process; these results are comparable to the results from Ahn et al.

To compare the resistivity of TiN using thermal ALD with different precursors, the benchmarking of the TiN ALD is shown in Figure 8. Temperature is a critical factor that directly affects the resistivity of TiN. It is hypothesized that at higher temperatures, better crystallinity could be achieved, resulting in low resistivity. Among all halogen-free precursors, the thermal stability of TEMATi is the greatest, enabling this precursor to


https://doi.org/10.1021/acsaelm.3c00245
ACS Appl. Electron. Mater. XXXX, XXX, XXX−XXX

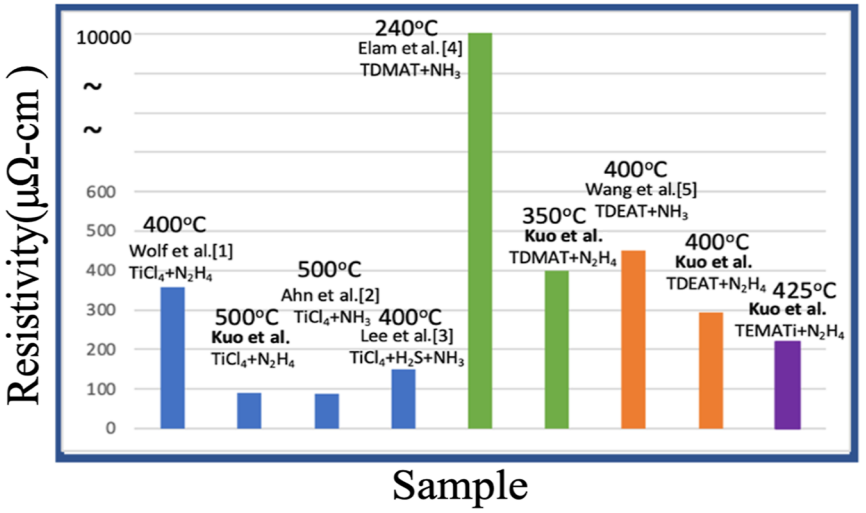


**Figure 8.** Benchmark of TiN using different precursors (blue: $TiCl_4$; green: TDMAT; orange: TDEAT; and purple: TEMATi). For the results reported in the present study, the thickness of the thin films was around 15 nm to ensure that surface oxidation effects are minimal. Note that temperature plays an important role in terms of resistivity.

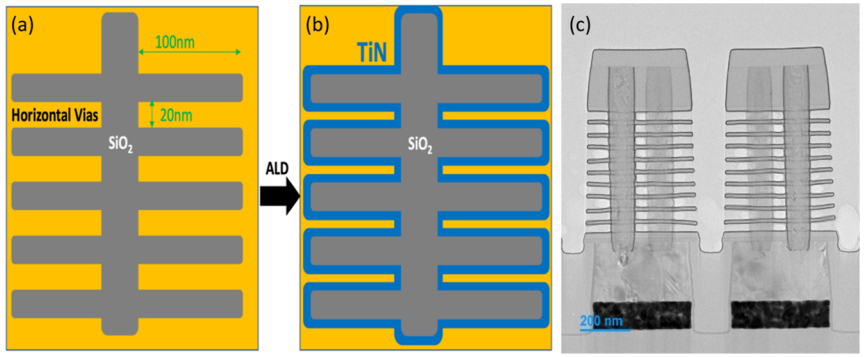


**Figure 9.** Illustration of the growth of TiN (blue region) in the horizontal vias in a pattern before (a) and after (b) the ALD deposition. (c) Overview of the lamella of the patterned sample after the deposition using $TiCl_4$ and $N_2H_4$ at 425 °C. TiN thin films were deposited in the top region, horizontal vias, and the bottom parts of the patterned structure (thin black lines in the TEM image). The aspect ratio of the horizontal vias is 5:1. A few fins were bent during the sample preparation by FIB.

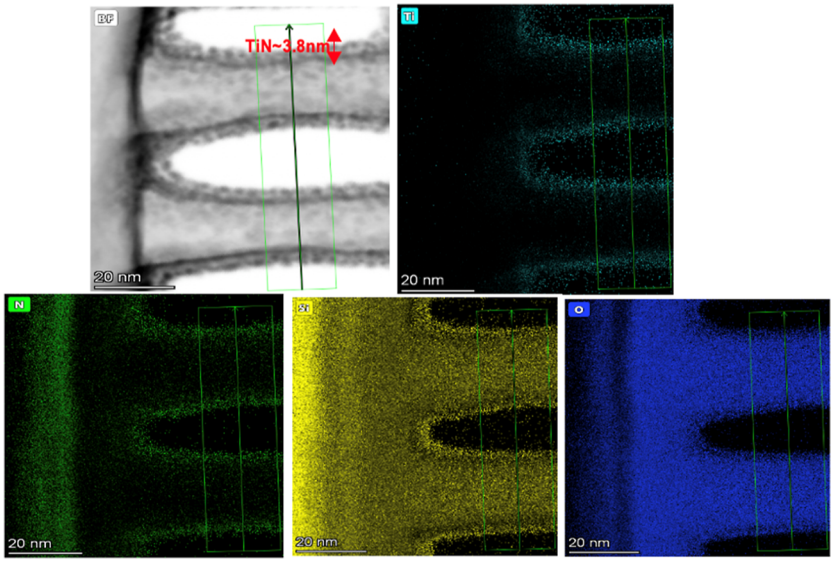


**Figure 10.** BF-TEM and EDX of TiN using $TiCl_4$ and $N_2H_4$ in the horizontal vias at 425 °C. BF-TEM shows that the thickness of TiN in the horizontal vias is around 3.8 nm. EDX mapping in the green rectangular region confirms the presence of the TiN thin film. The fins are $SiO_2$.


https://doi.org/10.1021/acsaelm.3c00245
ACS Appl. Electron. Mater. XXXX, XXX, XXX−XXX

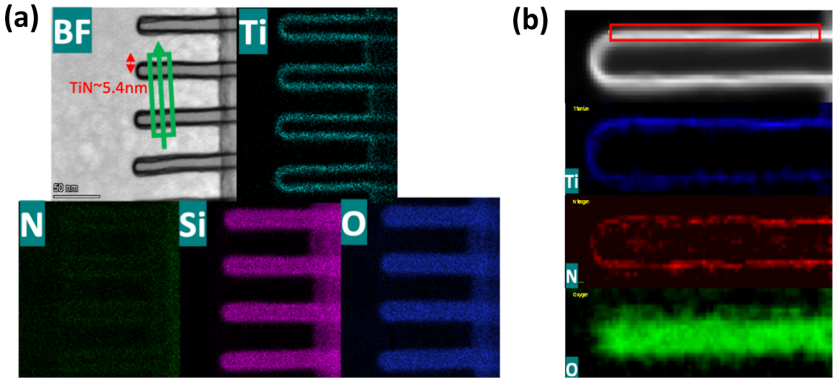


**Figure 11.** (a) BF-TEM and EDX of TiN using TEMATi and $N_2H_4$ in the horizontal vias at 425 °C. (b) EELS of TiN in the red rectangular region. Ti and N were qualitatively analyzed through EELS. However, the nitrogen signal was not strong enough to quantitatively calculate the chemical composition of the thin film in the horizontal vias.

be employed at a higher temperature compared to the other precursors, consistent with its lower resistivity compared to all other organic precursors.

Patterned samples with horizontal vias were used to verify the conformality of the low-resistivity TiN deposition processes. Figure 9a shows a cross-sectional diagram of the structure of horizontal vias in the patterned samples. The fin structure is made of $SiO_2$ with an aspect ratio of 5:1. TiN thin films were deposited in the horizontal vias by thermal ALD, which is shown by the blue region in the middle figure. A cross-sectional TEM image after deposition is shown in Figure 9c for $TiCl_4$ and $N_2H_4$ at 425 °C.

A high-conformality TiN thin film (~3.8 nm) was deposited in horizontal vias using $TiCl_4$ + $N_2H_4$ at 425 °C, as demonstrated by the TEM with EDX mapping shown in Figure 10. Bright-field transmission electron microscopy (BF-TEM) of the fins at the thinner edge of the lamella is shown. EDX mapping in the green rectangular region shows that the fins were $SiO_2$ and the thin film that was conformally grown in the horizontal vias was $TiO_xN_y$. Note that the films were exposed to the atmosphere for several days for the FIB sample preparation and TEM analysis; therefore, the very thin deposited TiN was oxidized to $TiO_xN_y$ which was observed in the TEM/EDX.

A high-conformality TiN thin film (~5.4 nm) was deposited in horizontal vias using a halogen-free process: TEMATi + $N_2H_4$ at 425 °C (see Figure 11). The BF-TEM images show that TiN with a high contrast compared to the fins was conformally deposited in the horizontal vias. EDX mapping of the green region indicates that TiN is grown in the horizontal vias although the signal of nitrogen is weak, which is due to the oxidation during the sample preparation and TEM analysis. To further confirm the chemical composition, EELS was utilized to confirm the existence of TiN in the horizontal vias, which is shown in Figure 11b. In the red rectangular region, chemical composition was qualitatively analyzed by EELS. The signal of the nitrogen was too weak to get quantitative results, which was probably due to the surface oxidation of the thin film. The data is consistent with TiN thin films being conformally grown by halogen-free ALD in the patterned sample by using TEMATi and $N_2H_4$ at 425 °C; this process is suitable for 3D NAND high aspect ratios of 5:1.

## SUMMARY

TiN thin films with record low resistivity at 500 °C were deposited by halogen-based ALD. Surface impurities such as oxygen and chlorine will increase the resistivity. By increasing the exposure to a highly reactive nitrogen source, $N_2H_4$, the oxygen content in the TiN thin films could be suppressed. Several metal−organic precursors such as TDMAT, TDEAT, and TEMATi were tested. By minimizing the pulse length of the Ti precursor, the surface carbon content was reduced. The metal−organic Ti precursor with the highest thermal stability is required to deposit the ALD TiN films with the lowest resistivity. ALD using TEMATi at 425 °C deposited TiN films with both the lowest carbon content and lowest resistivity (~220 $\mu\Omega$ cm) compared to other metal−organic Ti precursors. For the conformality test, TEM was applied to examine the growth of TiN in the horizontal vias of the patterned substrates. Conformal TiN was deposited in the vias with 3.8 and 5.4 nm by using $TiCl_4$ and TEMATi at 425 °C.

## ASSOCIATED CONTENT

### Supporting Information

The Supporting Information is available free of charge at https://pubs.acs.org/doi/10.1021/acsaelm.3c00245.

Self-limiting study of TiN using $TiCl_4$ and other metal−organic precursors and density and roughness studies at different temperatures (PDF)

## AUTHOR INFORMATION

### Corresponding Author

**Andrew C. Kummel** − *Department of Chemistry and Biochemistry, University of California, San Diego, California 92093, United States;* orcid.org/0000-0001-8301-9855; Email: akummel@ucsd.edu

### Authors

**Cheng-Hsuan Kuo** − *Materials Science and Engineering Program, University of California, San Diego, California 92093, United States;* orcid.org/0009-0005-5387-8882

**Aaron J. Mcleod** − *Department of Chemistry and Biochemistry, University of California, San Diego, California 92093, United States;* orcid.org/0000-0002-3720-0992

**Ping-Che Lee** − *Materials Science and Engineering Program, University of California, San Diego, California 92093, United States*



https://doi.org/10.1021/acsaelm.3c00245
ACS Appl. Electron. Mater. XXXX, XXX, XXX−XXX

**James Huang** − *Materials Science and Engineering Program, University of California, San Diego, California 92093, United States;* orcid.org/0000-0003-3279-0783
**Harshil Kashyap** − *Materials Science and Engineering Program, University of California, San Diego, California 92093, United States;* orcid.org/0000-0003-3845-6110
**Victor Wang** − *Materials Science and Engineering Program, University of California, San Diego, California 92093, United States;* orcid.org/0000-0003-1544-2154
**SeongUK Yun** − *Department of Chemistry and Biochemistry, University of California, San Diego, California 92093, United States;* orcid.org/0000-0002-1821-6753
**Zichen Zhang** − *Materials Science and Engineering Program, University of California, San Diego, California 92093, United States;* orcid.org/0000-0001-8028-3271
**Jeffrey Spiegelman** − *Rasirc, San Diego, California 92093, United States*
**Ravindra Kanjolia** − *EMD Electronics, Haverhill, Massachusetts 01832, United States*
**Mansour Moinpour** − *EMD Electronics, Haverhill, Massachusetts 01832, United States*

Complete contact information is available at: https://pubs.acs.org/10.1021/acsaelm.3c00245

### Notes

The authors declare no competing financial interest.

## ■ ACKNOWLEDGMENTS

CHIMES, Center for Heterogeneous Integration of Micro Electronic Systems, one of six centers in the Joint University Microelectronics Program (JUMP2.0), a Semiconductor Research Corporation (SRC) program sponsored by the Defense Advanced Research Projects Agency (DARPA). This work was performed in part at the San Diego Nanotechnology Infrastructure (SDNI) at UC San Diego, a member of the National Nanotechnology Coordinate Infrastructure, which is supported by the National Science Foundation (ECCS-1542148).

## ■ REFERENCES

(1) Elers, K. E.; Saanila, V.; Soininen, P. J.; Li, W. M.; Kostamo, J. T.; Haukka, S.; Juhanoja, J.; Besling, W. F. A. Diffusion Barrier Deposition on a Copper Surface by Atomic Layer Deposition. *Chem. Vap. Deposition* **2002**, *8*, 149−153.
(2) Mändl, M.; Hoffmann, H.; Kücher, P. Diffusion Barrier Properties of Ti/TiN Investigated by Transmission Electron Microscopy. *J. Appl. Phys.* **1990**, *68*, 2127−2132.
(3) Baumann, J.; Werner, T.; Ehrlich, A.; Rennau, M.; Kaufmann, C.; Gessner, T. TiN Diffusion Barriers for Copper Metallization. *Microelectron. Eng.* **1997**, *37*−*38*, 221−228.
(4) Sidhwa, A.; Spinner, C.; Gandy, T.; Brown, W.; Ang, S.; Naseem, H.; Ulrich, R. Evaluation of Contact and Via Step Coverage Using a Novel Two-Step Titanium Nitride Barrier Deposition Process. *Mater. Res. Soc.* **2002**, *716*, B12.10.1−B12.10.6.
(5) Whang, S.; Joo, M.; Seo, B.; Chang, K.; Kim, W.; Jung, T.; Kim, G.; Lim, J.; Kim, K.; Hong, K.; Park, S. Thermally Stable Ni-Silicide Gate Electrode with TiN Barrier Metal for NAND Flash Memory Application with 24 Nm Technology and Beyond. *Extended Abstracts of the 2009 International Conference on Solid State Devices and Materials*; The Japan Society of Applied Physics: Sendai, 2009; pp 48−49.
(6) Ho, C. Y.; Chang, Y. J.; Chiou, Y. L. Enhancement of Programming Speed on Gate-All-around Poly-Silicon Nanowire Nonvolatile Memory Using Self-Aligned NiSi Schottky Barrier Source/Drain. *J. Appl. Phys.* **2013**, *114*, 054503.
(7) Kao, E.; Yang, C.; Warren, R.; Kozinda, A.; Lin, L. ALD Titanium Nitride Coated Carbon Nanotube Electrodes for Electrochemical Supercapacitors. In *2015 Transducers—2015 18th International Conference on Solid-State Sensors, Actuators and Microsystems, TRANSDUCERS 2015*; Institute of Electrical and Electronics Engineers Inc., 2015; pp 498−501. .
(8) Zgrabik, C. M.; Hu, E. L. Optimization of Sputtered Titanium Nitride as a Tunable Metal for Plasmonic Applications. *Opt. Mater. Express* **2015**, *5*, 2786.
(9) Ahn, C. H.; Cho, S. G.; Lee, H. J.; Park, K. H.; Jeong, S. H. Characteristics of TiN Thin Films Grown by ALD Using $TiCl_4$ and $NH_3$. *Met. Mater. Int.* **2001**, *7*, 621−625.
(10) Umoren, S. A.; Solomon, M. M. Effect of Halide Ions on the Corrosion Inhibition Efficiency of Different Organic Species—A Review. *J. Ind. Eng. Chem.* **2015**, *21*, 81−100.
(11) Piallat, F.; Gassilloud, R.; Caubet, P.; Vallée, C. Investigation of TiN Thin Film Oxidation Depending on the Substrate Temperature at Vacuum Break. *J. Vac. Sci. Technol., A* **2016**, *34*, 051508.
(12) Kröger, R.; Eizenberg, M.; Marcadal, C.; Chen, L. Plasma Induced Microstructural, Compositional, and Resistivity Changes in Ultrathin Chemical Vapor Deposited Titanium Nitride Films. *J. Appl. Phys.* **2002**, *91*, 5149−5154.
(13) Stevens, E.; Tomczak, Y.; Chan, B. T.; Altamirano Sanchez, E.; Parsons, G. N.; Delabie, A. Area-Selective Atomic Layer Deposition of TiN, TiO2, and HfO2 on Silicon Nitride with Inhibition on Amorphous Carbon. *Chem. Mater.* **2018**, *30*, 3223−3232.
(14) Elers, K. E.; Winkler, J.; Marcus, S. TiCl4, as a Precursor in the TiN Deposition by ALD and PEALD. *Proc.—Electrochem. Soc.* **2004**, *1*, 361−368.
(15) Wolf, S.; Breeden, M.; Kwak, I.; Park, J. H.; Kavrik, M.; Naik, M.; Alvarez, D.; Spiegelman, J.; Kummel, A. C. Low Temperature Thermal ALD TaN x and TiN x Films from Anhydrous N 2 H 4. *Appl. Surf. Sci.* **2018**, *462*, 1029−1035.
(16) Lee, H. J.; Hwang, J. H.; Park, J. Y.; Lee, S. W. Alternative Surface Reaction Route in the Atomic Layer Deposition of Titanium Nitride Thin Films for Electrode Applications. *ACS Appl. Electron. Mater.* **2021**, *3*, 999−1005.
(17) Elam, J. W.; Schuisky, M.; Ferguson, J. D.; George, S. M. Surface Chemistry and Film Growth during TiN Atomic Layer Deposition Using TDMAT and NH3. *Thin Solid Films* **2003**, *436*, 145−156.
(18) Wang, L.; Liu, B.; Song, Z.; Feng, S.; Zhou, Z.; Xiang, Y.; Zhang, F. Atomic Vapor Deposition of TiN with Diluted Tetrakis (Diethylamido) Titanium (TDEAT) for Phase Change Memory. *ECS Trans.* **2009**, *22*, 167−173.
(19) Kim, J. Y.; Choi, G. H.; Kim, Y. D.; Kim, Y.; Jeon, H. Comparison of TiN Films Deposited Using Tetrakisdimethylaminotitanium and Tetrakisdiethylaminotitanium by the Atomic Layer Deposition Method. *Jpn. J. Appl. Phys., Part 1* **2003**, *42*, 4245−4248.
(20) Musschoot, J.; Xie, Q.; Deduytsche, D.; Van den Berghe, S.; Van Meirhaeghe, R. L.; Detavernier, C. Atomic Layer Deposition of Titanium Nitride from TDMAT Precursor. *Microelectron. Eng.* **2009**, *86*, 72−77.
(21) Lee, Y. J. Low-impurity, highly conformal atomic layer deposition of titanium nitride using NH3−Ar−H2 plasma treatment for capacitor electrodes. *Mater. Lett.* **2005**, *59*, 615−617.
(22) Faraz, T.; Knoops, H. C. M.; Verheijen, M. A.; Van Helvoirt, C. A. A.; Karwal, S.; Sharma, A.; Beladiya, V.; Szeghalmi, A.; Hausmann, D. M.; Henri, J.; Creatore, M.; Kessels, W. M. M. Tuning Material Properties of Oxides and Nitrides by Substrate Biasing during Plasma-Enhanced Atomic Layer Deposition on Planar and 3D Substrate Topographies. *ACS Appl. Mater. Interfaces* **2018**, *10*, 13158−13180.
(23) Chen, Z. X.; Li, X.; Li, W.-M.; Lo, G.-Q. Plasma-Enhanced Atomic Layer Deposition (PEALD) of TiN Using the Organic Precursor Tetrakis(Ethylmethylamido)Titanium (TEMAT). *2015 2nd International Conference on Chemical and Material Engineering (ICCME 2015)*; {EDP} Sciences, 2016.

(24) Yun, J.-Y.; Park, M.-Y.; Rhee, S.-W. Comparison of Tetrakis-(Dimethylamido)Titanium and Tetrakis(Diethylamido)Titanium as Precursors for Metallorganic Chemical Vapor Deposition of Titanium Nitride. *J. Electrochem. Soc.* **1999**, *146*, 1804−1808.
(25) Seong, J. K.; Kim, B. H.; Woo, H. G.; Kim, S. K.; Kim, D. H. Thermal Decomposition of Tetrakis(Ethylmethylamido) Titanium for Chemical Vapor Deposition of Titanium Nitride. *Bull. Korean Chem. Soc.* **2006**, *27*, 219−223.
(26) Chawla, J. S.; Zhang, X. Y.; Gall, D. Effective Electron Mean Free Path in TiN(001). *J. Appl. Phys.* **2013**, *113*, 063704.



https://doi.org/10.1021/acsaelm.3c00245
*ACS Appl. Electron. Mater.* XXXX, XXX, XXX−XXX